Sakarya Üniversitesi Fen Bilimleri Dergisi
Sakarya University Journal of Science

e-ISSN : 2147-835X
Publisher : Sakarya University

Vol. 29, No. 4, 383-401, 2025
DOI: https://doi.org/10.16984/saufenbilder.1646947

Research Article

# DFT Calculations, ADME Analysis and Molecular Docking Studies of the Compound AHTPO With the Digestive Enzyme Trypsin Found in Cold-Adapted Fish Species

Erdi Anıl Tanrıverdi[1], Aslıhan Aycan Tanrıverdi[2*], Ümit Yıldıko[3]

[1] Bayburt University, Health Services Vocational School, Department of Medical Services and Techniques, Bayburt, Türkiye, eatanriverdi@bayburt.edu.tr, ror.org/050ed7z50
[2] Kafkas University, Faculty of Science and Letters, Department of Chemistry, Kars, Türkiye, t.aslihanaycan@gmail.com, ror.org/04v302n28
[3] Kafkas University, Faculty of Engineering and Architecture, Department of Bioengineering, Kars, Türkiye, yildiko1@gmail.com, ror.org/04v302n28
*Corresponding Author

ARTICLE INFO

Keywords:
Thiazolo
Pyrimidine
DFT
Molecular docking
Trypsin

Article History:
Received: 25.02.2025
Revised: 04.07.2025
Accepted: 24.07.2025
Online Available: 11.08.2025

ABSTRACT

For the special amine 7-Amino-3-(4-aminophenyl)-5H-thiazolo[3,2-a]pyrimidin-5-one (AHTPO), previously reported experimental biological activities served as the foundation for further studies. Computational chemistry and molecular simulation techniques were subsequently applied to investigate AHTPO. Its interactions with trypsin enzymes derived from cold-adapted fish species were examined. The compound's biological activity and pharmacokinetic properties were assessed using DFT calculations, molecular docking, and ADME analyses. Molecular docking results indicated that AHTPO exhibits strong binding affinities with the 1A0J and 2TBS enzymes, with the binding to 2TBS being energetically more favorable. Additionally, ADME analysis revealed that while the AHTPO shows potential for pharmaceutical applications, its gastrointestinal absorption and blood-brain barrier permeability may present certain limitations. Regarding its electronic and optical properties, AHTPO's high dipole moment and polarizability values enhance its flexibility and adaptability in biological environments. The HOMO-LUMO energy gap suggests that the AHTPO achieves a balance between stability and reactivity, enabling high activity in biomolecular interactions. These findings highlight the promising pharmacological potential of AHTPO in binding with trypsin enzymes, suggesting its viability as a therapeutic agent.

## 1. Introduction

The synthesis of 7-Amino-3-(4-aminophenyl)-5H-thiazolo[3,2-a]pyrimidin-5-one (AHTPO)[1] was achieved through a one-pot procedure using S-alkylated thiouracils in concentrated $H_2SO_4$ at 80°C via an intramolecular cyclization/sulfonation sequence. Interestingly, under ambient conditions, S-alkylated thiouracil only underwent intramolecular cyclization, leading to the formation of a corresponding amine derivative. The synthesized compound AHTPO was evaluated for in vitro antibacterial activity against two Gram-positive bacterial strains—*Staphylococcus aureus* (S. aureus) and *Bacillus subtilis* (*B. subtilis*)—as well as two Gram-negative bacterial strains—*Escherichia coli* (*E. coli*) and *Pseudomonas aeruginosa* (*P. aeruginosa*).

Antibacterial efficacy was evaluated using the broth microdilution method, a widely accepted standard for determining minimum inhibitory concentrations (MICs)[1]. The reported minimum inhibitory concentration (MIC) values for antibacterial activity were as follows: 800 µg/mL for *S. aureus*, 400 µg/mL for *B. subtilis*, 400 µg/mL for *E. coli*, and 100 µg/mL for *P. aeruginosa*. Previous screening data (Cai et al., 2016) revealed that AHTPO demonstrated

**Cite as:** E. A. Tanrıverdi, A. A. Tanrıverdi, Ü. Yıldıko, "DFT calculations, ADME analysis and molecular docking studies of the compound AHTPO with the digestive enzyme trypsin found in cold-adapted fish species," Sakarya University Journal of Science, vol. 29, no. 4, pp. 383-401, 2025. https://doi.org/10.16984/saufenbilder.1646947

stronger activity against Gram-negative bacteria than against Gram-positive strains. Furthermore, the presence of a primary amino substitution in the phenyl group of AHTPO contributed to its moderate efficacy against *P. Aeruginosa* [1].

Trypsin is a well-characterized serine protease, widely studied due to its fundamental role in digestion and protein hydrolysis. Many structures of trypsin and trypsinogen have been determined through X-ray crystallography. Except for agnathan trypsins, vertebrate trypsins are classified into one of two groups. Group I trypsins are typically anionic at physiological pH, while group II trypsins are generally cationic at physiological pH [2]. Most vertebrates possess at least one trypsinogen gene from each group. Due to the strong selective pressure to maintain the function of this universally important digestive enzyme, it is difficult to accurately estimate the evolutionary distance between vertebrate and invertebrate structures [2, 3]. As a result, invertebrate trypsin sequences cannot be reliably used for basic calculations of vertebrate trypsin phylogeny.

The first determined sequence, from *Pleuronectes platessa* (flounder), initially appeared to be a unique outlier. However, the subsequent identification of sequences from *Dissostichus mawsoni* (giant Antarctic toothfish), *Notothenia coriiceps* (black rock cod), *Pleuronectes americanus* (winter flounder), and *Paralichthys olivaceus* (bastard flounder) suggested the existence of a new trypsin clade. *P. platessa* and *P. americanus* are Arctic-boreal fishes that migrate between sub-zero Arctic waters and warmer waters. *P. olivaceus*, a demersal fish, is not an Arctic resident, but like Pleuronectes species, it must cope with the low temperatures of the ocean depths, similar to Gadus morhua [2, 4-6].

Molecular docking is a widely employed computational technique for predicting ligand-protein interactions and estimating binding affinities [7-9,10]. The results are typically evaluated based on criteria such as binding energy, with lower energy conformations being considered more stable. Molecular docking plays a crucial role in drug design, the study of biomolecular interactions, and toxicology research [11,12]. Additionally, several software tools are available for molecular docking, including popular options ,12such as AutoDock, Dock, Glide, and FlexX [13,14]. However, the accuracy of molecular docking can vary depending on factors such as protein flexibility, the quality of structural data, and computational power [15].

In the future, the accuracy and efficiency of molecular docking are expected to improve with the integration of technologies like artificial intelligence and machine learning. For the molecular docking studies of AHTPO, two trypsin enzymes were selected [16]. The first was a non-psychrophilic trypsin enzyme from a cold-adapted fish species, with the Protein Data Bank (PDB) ID: 1A0J [17] The second was a cold-adapted trypsin enzyme, identified as 2TBS [18]. The crystal structure of the 1A0J enzyme, cationic trypsin (CST) derived from Atlantic salmon (Salmo salar), was refined by Schrøder et al. at a resolution of 1.70 Å. Their study aimed to identify structural explanations for the differences in thermostability and catalytic efficiency between CST, anionic salmon trypsin (AST), and beef trypsin (BT) through comprehensive structural comparisons [17].

Meanwhile, the crystal structure of the 2TBS enzyme, representing an anionic form of salmon trypsin, was determined by Smalås et al. at a resolution of 1.82 Å. This research provided the first structural insights into a trypsin enzyme from a poikilothermic organism. A detailed comparison with mammalian trypsins was conducted to uncover structural adaptations that contribute to the cold adaptation properties of salmon trypsin. 1A0J and 2TBS represent structurally distinct isoforms of trypsin from cold-adapted fish species. 1A0J is a cationic variant, while 2TBS is an anionic isoform. These enzymes differ in their catalytic site dynamics, which influences their binding behavior under low-temperature physiological conditions. In particular, 2TBS is characterized by higher surface cycling flexibility, which contributes to cold adaptation [18].

Density Functional Theory (DFT) is a fundamental method in quantum chemistry that is widely used to solve the electronic structure of

molecules and solids [19]. DFT is based on the calculation of the energy levels and electron density of a system, and it is particularly powerful for understanding chemical reactions, molecular properties, and matter [20, 21]. This theory mathematically describes the interactions between electrons, allowing for the prediction of the total energy and properties of a system [22, 23].

Compared to more complex computational methods like Hartree-Fock, DFT requires less computational power, making it suitable for large systems. DFT has a broad range of applications in chemistry and materials science [24, 25]. It is commonly used in molecular dynamics simulations, molecular structure optimization, reactivity studies, and electronic structure analysis [26, 27]. Additionally, DFT plays a crucial role in the design of organic and inorganic compounds, drug discovery, photochemical processes, and catalytic reactions [28, 29]

In this article, computational chemistry and molecular simulation studies were performed for the AHTPO compound in light of the available experimental biological activities. AHTPO compound's interactions with trypsin enzymes obtained from cold-adapted fish species were closely investigated. The biological activity and pharmacokinetic properties of the compound were presented with DFT calculations, molecular docking, and ADME analyses. In terms of electronic and optical properties, AHTPO with high dipole moment and polarizability values stand out for its flexibility and molecular adaptability. The energy range confirms that the compound can exhibit high activity in biomolecular interactions by maintaining the balance of stability and reactivity. The biological binding potential of AHTPO with trypsin enzyme is promising as a pharmacological agent.

## 2. General Methods

### 2.1. Theoretical calculations

The molecular geometry of AHTPO was fully optimized using the DFT/B3LYP/6-311G(d,p) basis set, and the excited-state properties were evaluated via TD-DFT/CAM-B3LYP/6-31G. All quantum chemical calculations were performed with the Gaussian09 software package [30]. The B3LYP/6-311G(d,p) basis set was selected for the ground state optimization due to its reliable performance in geometry predictions. Considering its effectiveness in accounting for long-range charge transfer interactions, TD-DFT with CAM-B3LYP/6-31G was used for excited state calculations.

Additionally, molecular docking was performed to identify the precise binding site of the ligand on the protein and to elucidate its binding mechanism. The Schrödinger, LLC Maestro Molecular Modeling platform (version 11.8) was used for docking studies [31, 32], while the resulting receptor model and the predicted 2D and 3D interactions were analyzed using Discovery Studio (version 4.5) [33]. Protein structures (PDB IDs: 1A0J and 2TBS) were obtained from the RCSB Protein Data Bank. The Protein Preparation Wizard in Schrödinger Maestro (v11.8) was used for preprocessing. This included assigning bond orders, adding hydrogen atoms, correcting protonation states at pH 7.4, and optimizing hydrogen bond networks. Binding sites were identified based on the coordinates of co-crystallized ligands. The ADME (absorption, distribution, metabolism, and excretion) parameters were computed using the ADME 3.0 web server [34]. The molecule's SMILES format was uploaded to estimate various physiological and pharmacokinetic properties, and the results were thoroughly analyzed [35].

## 3. Results and Discussion

### 3.1. Density functional theory system

The DFT system can provide valuable insights for studying the biological activity effects of the AHTPO compound (Figure 1). The adsorption of a compound onto a metal surface is likely influenced by its inhibitory effects. In this process, one of the interacting species serves as an electron pair acceptor, while the other acts as an electron pair donor [36, 37].

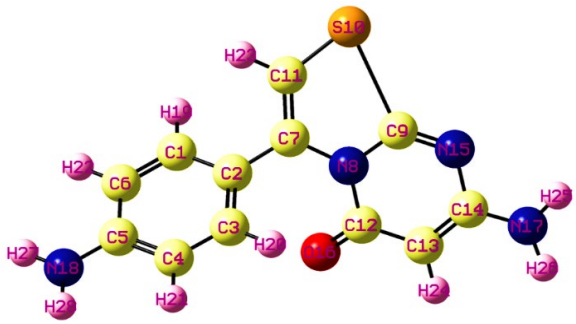

**Figure 1.** The 3D position of the composite AHTPO in space was obtained

### 3.1.1. Dipole moment and UV-visible

The determination of the dipole moments of the AHTPO molecule in its excited state is essential for understanding the solvent dependence of its electronic spectra [38-40]. The excited electronic wave function and polarization can be evaluated using the theoretically calculated dipole moments. The polarity functions of the AHTPO compound are presented in Table 1. The ground-state dipole moment and the changes in the dipole moments of the compound are determined using appropriate equations. Ground-state analysis of the thiazole ring suggests that the observed dipole moment is primarily driven by internal charge transfer arising from uneven electron distribution.

As shown in Table 1, the dipole moment calculated using the DFT/B3LYP-6-311G(d,p) basis set is larger than that obtained with the TD-DFT/CAM-B3LYP-6-31G basis set. This suggests that AHTPO is polar and more sensitive to its solvent environment. During the electronic transition process, the polarity parameter method, which accounts for specific solute-solvent interactions, produces the largest dipole moment value [41]. Equations (1, 2, and 3) [42] are as follows, respectively:

**Table 1.** Dipole moments (μ (D)), polarizability (α (au)), and Hyperpolarizability (β (esu)) values were calculated for two different systems

| Parameters | DFT/B3LYP-6-311G(d,p) | TD-DFT/CAM-B3LYP-6-31G | Parameters | DFT/B3LYP-6-311G(d,p) | TD-DFT/CAM-B3LYP-6-31G |
|---|---|---|---|---|---|
| $\mu_x$ | -6.3113 | -0.4142 | $\beta_{XXX}$ | -156.6579 | -10.2748 |
| $\mu_y$ | -4.5388 | 0.1304 | $\beta_{XXY}$ | -145.6844 | -105.7119 |
| $\mu_z$ | 2.2884 | -0.6783 | $\beta_{XYY}$ | -3.7540 | 10.4316 |
| **μ (D)** | 8.1037 | 0.8054 | $\beta_{YYY}$ | -77.5625 | -2.2126 |
| $\alpha_{xx}$ | -51.6568 | -78.4706 | $\beta_{XXZ}$ | 15.6357 | -56.9963 |
| $\alpha_{yy}$ | -109.0300 | -105.4068 | $\beta_{XYZ}$ | 17.4935 | 22.5872 |
| $\alpha_{zz}$ | -115.4202 | -111.1694 | $\beta_{YYZ}$ | 10.0779 | 1.9381 |
| $\alpha_{XY}$ | -19.3529 | -3.6310 | $\beta_{XZZ}$ | -5.6007 | -10.3474 |
| $\alpha_{XZ}$ | -2.0983 | 0.2232 | $\beta_{YZZ}$ | -1.3962 | -4.8855 |
| $\alpha_{YZ}$ | -12.2759 | -3.2241 | $\beta_{ZZZ}$ | 4.3554 | -2.2713 |
| **α (au)** | 108.1869 | 139.2368 | **β (esu)** | $3.55\ 10^{-34}$ | $7.57x\ 10^{-34}$ |

(The dipole moment (μ), polarizability (α), and hyperpolarizability (β) values calculated for AHTPO using two different basis sets. The significantly higher dipole moment observed in the DFT/B3LYP calculation suggests stronger solvent interactions and potential for stable enzyme binding in polar environments.)

The table presents the quantum chemical parameters of the AHTPO compound docked with the trypsin enzyme from a cold-adapted fish. These parameters include the dipole moment, polarizability (α), and hyperpolarizability (β) (Table 1). The dipole moment (μ) is 8.1037 Debye in the DFT/B3LYP-6-311G(d,p) set and 0.8054 Debye in the TD-DFT/CAM-B3LYP-6-31G set. This indicates that, in the first set, the electronic charge distribution of the molecule is asymmetric, resulting in a strong dipole.

When examining polarizability (α), the average value is calculated as 108.1869 a.u. in the DFT/B3LYP-6-311G(d,p) set, while the average value is 139.2368 a.u. in the TD-DFT/CAM-B3LYP-6-31G set. In the second set, higher polarizability is observed, meaning that AHTPO is more flexible and sensitive in its interaction with the trypsin protein. This increased flexibility

facilitates molecular adaptations during the binding process. Hyperpolarizability (β) values were found to be 3.55 x $10^{-34}$ esu and 7.57x$10^{-34}$ esu in the respective sets.

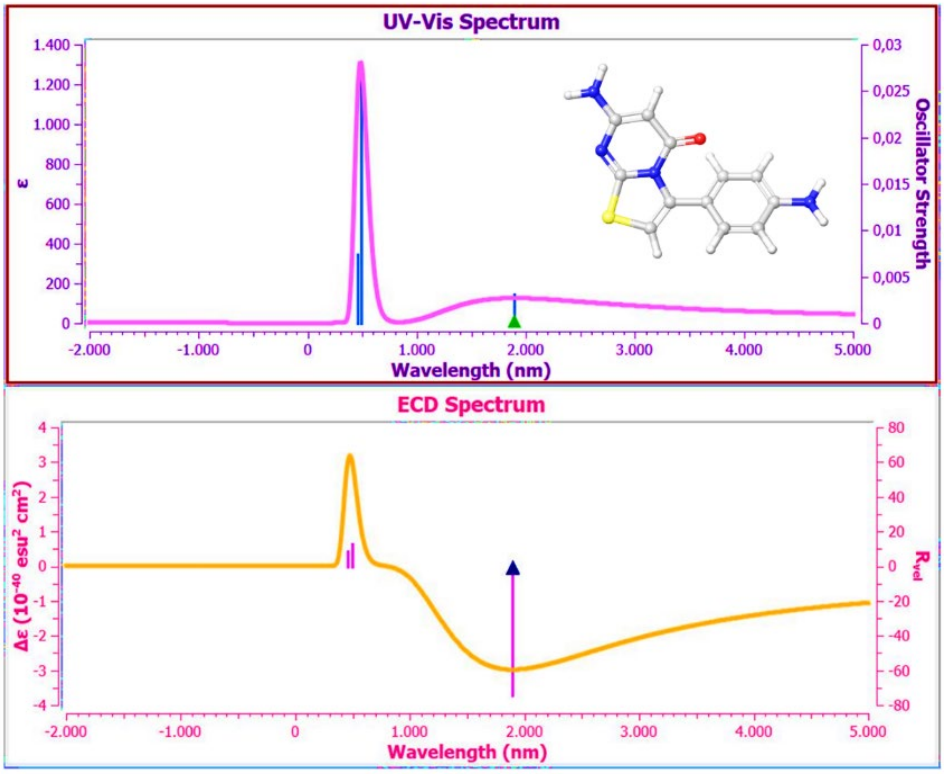


**Figure 1.** The UV-visible and ECD theoretical spectra of the compound AHTPO were obtained from the TD-DFT system *(*The theoretical UV-Vis spectrum calculated using TD-DFT indicates a primary absorption band in the range of 453–492 nm, corresponding to π–π* transitions. This excitation range confirms the conjugated structure and suggests electronic delocalization, supporting the molecule's potential in biological interactions.)

According to the Dipole Moment DFT/B3LYP method, a high dipole moment indicates that the compound AHTPO has a more polar structure [43]. In cold environments, a higher dipole moment allows the compound to establish stronger interactions with water molecules, which positively affects its biological activities, such as binding to enzymes or solubility. As observed, the polarizability value calculated with TD-DFT is higher, indicating that AHTPO is more sensitive to electric fields. This sensitivity will influence dynamic interactions in biological systems, as different polarization conditions may exist in an enzymatic environment.

High β values also suggest that AHTPO possesses non-linear optical (NLO) properties. While NLO does not directly affect the biological context, it can influence binding affinities and molecular interactions during molecular docking. These parameters enhance the functionality of AHTPO in biological systems and provide valuable insights for potential therapeutic or biotechnological applications. In the binding to the trypsin enzyme of a cold-adapted fish, the polarization effects will naturally determine the binding affinity and stability of the molecule. According to the DFT results, the order of polarization along the axes is αzz > αyy > αxx, meaning AHTPO is more polarized along the z-axis. Greater polarization along a specific axis indicates stronger interaction potential with biological targets during binding. Trypsin binds to substrates through hydrogen bonds and electrostatic interactions, and high dipole moment and polarizability can enhance the compound's ability to form these bonds with the enzyme. In cold environments, molecular interactions may occur more slowly; however, high dipole moments and polarizability will promote the rapid and stable binding of the molecule to the enzyme, ensuring that biochemical reactions proceed efficiently.

A Time-Dependent Density Functional Theory (TD-DFT) study was carried out at the B3LYP/6–311++G(d,p) level, and the calculated absorbances (λ) are presented in the graph. For the AHTPO compound, electron density depletion (red) and electron density increase (blue) are localized in the unsaturated rings and chains within the unit cell of the compound. The compound exhibits a single excitation level, with π to π* transitions occurring between 453 nm and 492 nm (Figure 2), spanning from the red to the green region. TD-DFT calculations only consider a small unit (unit cell) for the study. The bandwidth of TD-DFT calculations reflects values derived from the commonly used geometry, which results in a sharp shape for the theoretical spectrum [44].

### 3.1.2. FMO energies

The Frontier Molecular Orbital (FMO) analysis of the compound AHTPO involved determining the energy values of the Highest Occupied Molecular Orbital (HOMO) and the Lowest Unoccupied Molecular Orbital (LUMO). The energy gap between HOMO and LUMO provides insight into the molecule's reactivity and reflects its chemical stability [45, 46]. Using the DFT/B3LYP-6-311G(d,p) and TD-DFT/CAM-B3LYP-6-31G basis sets, the minimum energy gaps between HOMO and LUMO were calculated (Table 2 and Figure 3).

**Table 2.** The comparison HOMO, LUMO, energy gaps, etc., and properties of related FMO energies

| **Molecular Parameters** | **DFT/B3LYP-6-311G(d,p)** | **TD-DFT/CAM-B3LYP-6-31G** |
|---|---|---|
| $E_{HOMO}$ (eV) | -5.4470 | -6.1850 |
| $E_{LUMO}$ (eV) | -0.9818 | -2.6210 |
| $E_{HOMO-1}$ | -5.9101 | -7.7058 |
| $E_{LUMO+1}$ | -0.4620 | -0.2353 |
| Energy Gap[a] | 4.4652 | 3.5640 |
| Ionization Potential[b] | 5.4470 | 6.1850 |
| Electron Affinity[c] | 0.9818 | 2.6210 |
| Electronegativity[d] | 3.2144 | 4.4030 |
| Chemical Potential[e] | -3.2144 | -4.4030 |
| Chemical Hardness[f] | 2.2326 | 1.7820 |
| Chemical Softness[g] | 1.1163 | 0.8910 |
| Electrophilicity Index[h] | 2.3139 | 5.4395 |

[a] $(\Delta) = |E_{HOMO} - E_{LUMO}|$, [b] $I = -E_{HOMO}$, [c] $A = -E_{LUMO}$, [d] $\chi = (I + A)/2$, [e] $\mu = -(I + A)/2$, [f] $\eta = (I - A)/2$, [g] $S = 1/2\ \eta$, [h] $\omega = \mu^2/2\ \eta$

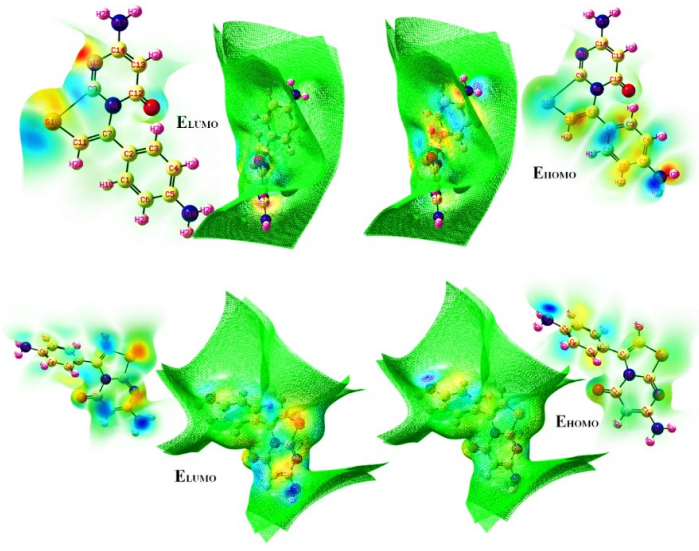


**Figure 3.** ESP HOMO-LUMO maps of compound AHTPO from different angles

When examining the molecular parameters in the table, the EHOMO and ELUMO energy levels, energy gap, ionization potential, electron affinity, electronegativity, chemical potential, chemical hardness/softness, and electrophilic index values were calculated using both TD-DFT and DFT methods. These values are crucial for understanding the electronic, optical, and biological properties of the AHTPO compound. For instance, there was a significant difference between the energy gap (3.5640 eV) calculated using the TD-DFT/CAM-B3LYP-6-31G method and the energy gap (4.4652 eV) calculated using the DFT/B3LYP-6-311G(d,p) method (Figure 4). This difference highlights the significant effect that different methods have on the reactivity and stability properties of the molecule.

Additionally, the lower EHOMO level obtained by the TD-DFT method suggests that the molecule has a higher ionization potential. These values are important indicators for understanding the chemical softness and hardness of the molecule. The energy gap is useful for predicting and analyzing the reactivity and biomolecular interaction capacity of AHTPO in biological environments. It should also be noted that in the energy gap of 3.5640 eV (TD-DFT), the molecule is stable in the enzyme environment but active in terms of electron transfer. From a biological and pharmacological perspective, a smaller energy gap indicates that the molecule is electronically more active and may tend to bind more strongly to its biological target.
This allows the compound AHTPO to adapt more easily during interaction with trypsin and form stronger bonds with the enzyme. From a pharmacological standpoint, this type of binding is directly related to the molecule's potential to modulate enzyme activity, bioavailability, and inhibitory effects. This energy gap value also suggests that the compound AHTPO is stable enough to remain intact within the enzyme, yet sufficiently active to interact. If this molecule were to be considered a pharmacological candidate, we could say that the potential for binding to the enzyme and regulating its activity is promising. Chemical hardness and softness provide valuable insights into the biological activity of a compound. These values are especially useful for understanding the stability and binding dynamics of AHTPO, particularly in its interaction with target proteins. The chemical hardness value reflects the compound's resistance to electron transfer. A high hardness value indicates that the molecule is more stable and less susceptible to reactive species.

According to the TD-DFT method, the hardness value of AHTPO, as shown in the table, was calculated to be 1.7820 eV. The biological significance of this value is that AHTPO can maintain its stability when exposed to high-energy or reactive species in the enzyme. This stability enables AHTPO to remain in the trypsin enzyme system for an extended period and interact more stably with the enzyme. The chemical softness value indicates the compound's susceptibility to polarization and electron sharing. A high softness value shows that AHTPO can more easily interact with biological targets. With a softness value of 0.8910 eV, the compound exhibits the potential to adapt to the active site of a specific biomolecule, such as trypsin. Pharmacologically, this softness suggests that AHTPO can provide conformational adaptation in trypsin, facilitating effective binding as an enzyme inhibitor.

By analyzing the HOMO (Highest Occupied Molecular Orbital) and LUMO (Lowest Unoccupied Molecular Orbital) values, more specific inferences can be made about the compound's reactivity in the biological system. According to the TD-DFT method, HOMO is related to the electron donation capacity. The HOMO value of -6.1850 eV indicates that the molecule is quite stable and resistant to oxidation. This suggests that AHTPO is less sensitive to high-energy molecules in the biological system. The ionization potential of 6.1850 eV supports this by indicating that AHTPO has a low tendency to lose an electron, allowing it to remain stable in a biological environment. The LUMO level relates to the compound's electron acceptability. With a value of -2.6210 eV, this shows that AHTPO has a moderate tendency to accept electrons. The compound's electron affinity of 2.6210 eV suggests it can interact with negatively charged compounds or electron-rich regions.

This property could facilitate interactions with enzyme systems, such as trypsin, that contain positively charged regions. The energy gap balances the molecule's stability in the biological environment with its chemical reactivity. The energy gap of 3.5640 eV indicates a reasonable level of reactivity for the compound. In other words, AHTPO can remain stable in the enzymatic trypsin system while still binding to the enzyme. From a pharmacological perspective, this energy gap suggests that AHTPO can exhibit appropriate activity in enzymatic systems without being overly reactive. Considering these values, it can be concluded that AHTPO can form a biological bond with the trypsin enzyme, and this bond will remain stable and controlled. The stability and controlled reactivity of AHTPO indicate that it holds promise as a pharmacological inhibitor or modülatör [47]. Descriptors such as moderate hardness and softness were revised to include quantitative values derived from HOMO-LUMO gap calculations. Additionally, for a comparative discussion referencing known pharmacological compounds to more clearly contextualize these descriptors in terms of chemical reactivity and biological interaction potential, see The calculated chemical hardness value of 1.7820 eV and softness of 0.8910 eV indicate a balanced reactivity. Compared to typical enzyme inhibitors with hardness values in the range of 1.5-2.0 eV, AHTPO lies in a favorable window for preserving molecular stability while maintaining interaction flexibility.

### 3.1.3. Molecular electrostatic potential maps and electrostatic surface potential maps

MEP (Molecular Electrostatic Potential) maps are an essential surface system for chemical structure analysis. MEP is based on electron density and helps to identify the locations of nucleophilic and electrophilic reactions. It provides valuable information about the types of chemical reactions a molecule can undergo (nucleophilic or electrophilic) and highlights the active sites for interactions. MEP surface mapping, which indicates both nucleophilic and electrophilic sites, is a practical method for observing the regioselectivity of a compound. Electrostatic potential is highest in red-colored regions and gradually decreases toward blue, representing a transition from nucleophilic to electrophilic sites. As indicated by this order, blue surfaces represent positive regions (electrophilic), while red and yellow surfaces correspond to nucleophilic regions (negative regions). Zero electrostatic potential surfaces (neutral regions) are green [40, 48]. The MEP maps for the AHTPO compound are shown in Figure 5.

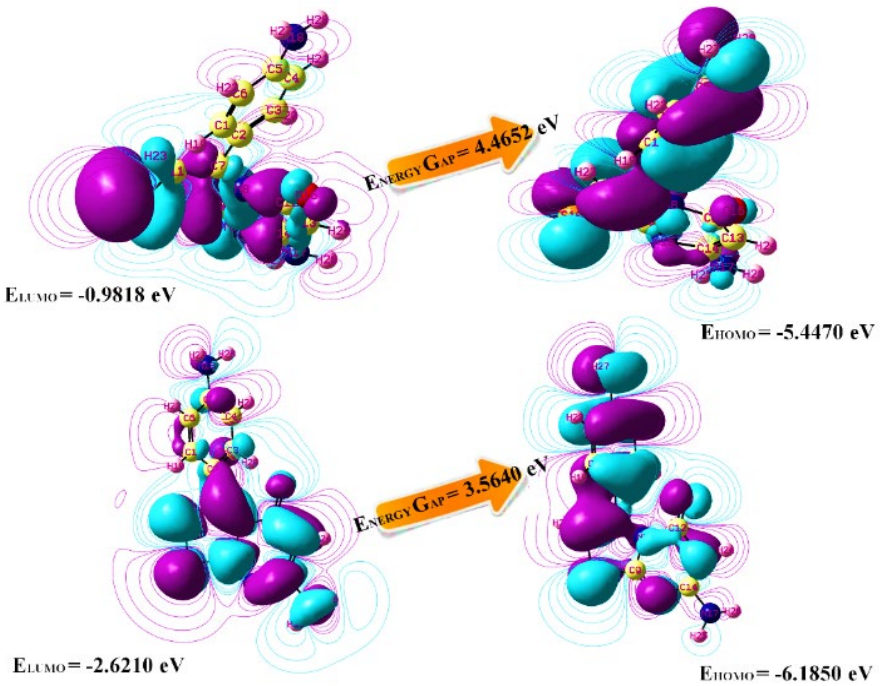


**Figure 4.** HOMO and LUMO energies of the compound AHTPO in DFT/B3LYP-6-311G(d,p) and TD-DFT/CAM-B3LYP-6-31G basis sets

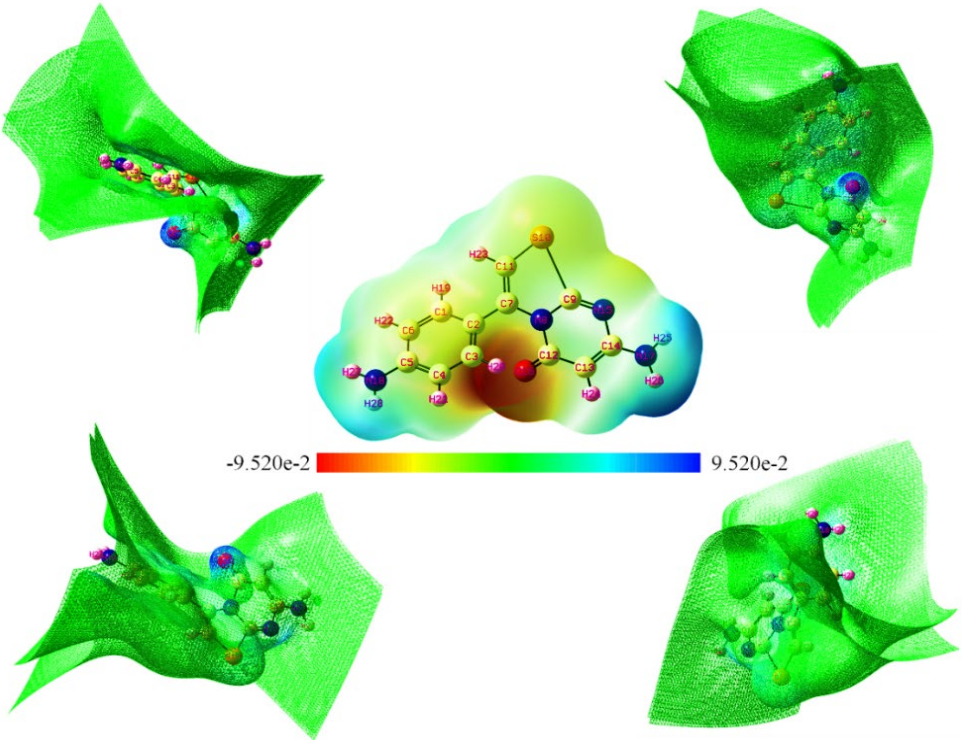


**Figure 5.** MEP and ESP maps of the compound AHTPO (DFT/B3LYP-6-311G(d,p)) (The nucleophilic (red) and electrophilic (blue) regions of AHTPO, which correspond to the ligand's observed binding orientation in the trypsin docking site.)

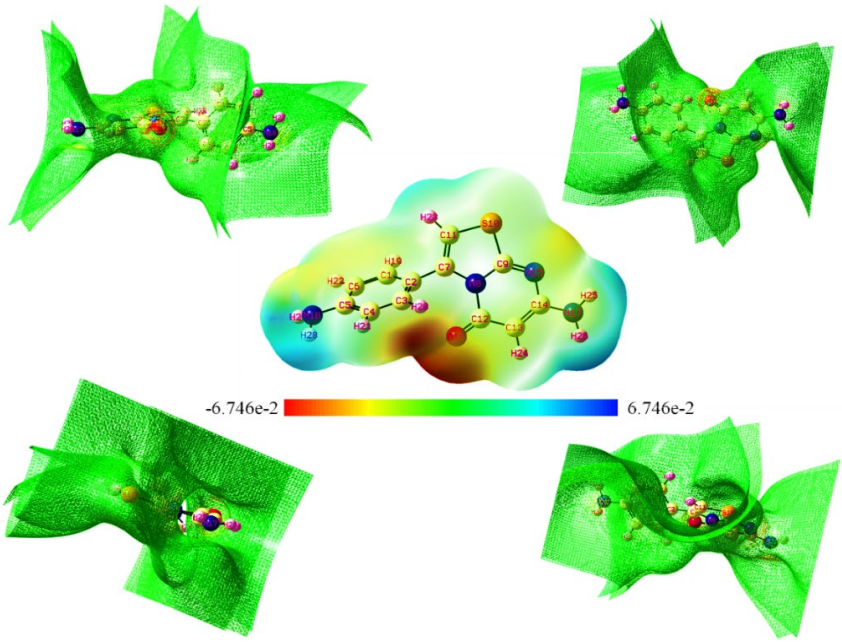


**Figure 6.** MEP and ESP maps of the compound AHTPO (TD-DFT/CAM-B3LYP-6-31G)

The outer envelope potential of the MEP related maps can be evaluated as the Electrostatic Surface Potential (ESP). These figures show the locations of positive and negative electrostatic potentials, the values range from $-9.520 \times 10^{-2}$ a.u. to $+9.520 \times 10^{-2}$ a.u. for Figure 6A and from $-6.746 \times 10^{-2}$ a.u. to $+6.746 \times 10^{-2}$ a.u. for Figure 6B. Based on these results, the MEP surface map shows negative potential regions around oxygen and nitrogen atoms and positive MEP surface regions around hydrogen atoms. The surface potential values were notably reduced in TD-DFT compared to DFT results.

AHTPO demonstrated favorable electronic properties, including a dipole moment of 8.10

Debye and polarizability values ranging from 108 to 139 a.u. The HOMO–LUMO energy gap values of 3.56 eV (TD-DFT) and 4.47 eV (DFT) indicate a balance between molecular stability and reactivity. The calculated chemical hardness (1.78 eV) and softness (0.89 eV) suggest that AHTPO maintains structural integrity while remaining flexible enough to interact efficiently with biological targets. These findings support the compound's suitability for enzyme binding under physiological conditions.

### 3.2. Molecular docking studies

#### 3.2.1. Glide scores in trypsin enzyme with

Molecular docking analysis was performed to investigate the interaction between 1A0J, 2TBS, and two primary targets (AHTPO and two trypsin enzymes) identified in the network. The scoring equation took into account various effects, such as electrostatic interactions, van der Waals forces, hydrogen bond contributions, and intermolecular conflicts. The studies confirmed that the free-binding energy was negative, indicating the formation of stable complexes. The binding energy was lower than the binding probability of the ligand to the receptor [29, 49, 50]. The results showed that the binding energies were strongly associated with the 1A0J/AHTPO and 2TBS/AHTPO complexes, with both primary target proteins. 2TBS formed four hydrogen bonds with ASP-122 and ASP-120 in the docking pocket of AHTPO. These essential targets may play a critical role in the molecular mechanism of ingestion toxicity induced by 1A0J and 2TBS.

The combination of antibacterial activity and molecular docking harnesses advances in bioinformatics, genomics, and big data to explore the mechanisms of mixed environmental pollutants. This methodology enhances the efficiency of ecotoxicological research. However, current studies, including this one, are limited to computer-aided techniques for understanding the molecular events behind the ingestion toxicity of 1A0J and 2BTS. These findings need to be validated through clear physiological animal experiments or clinical trials. In molecular docking, research can only theoretically predict the toxic targets of the compounds.

The docking scores resulting from the interactions of 1A0J and 2TBS enzymes with their natural ligands are -7.838 and -7.604 respectively.

There are significant differences between the 1A0J/AHTPO and 2TBS/AHTPO interactions. In the 1A0J/AHTPO interaction (Figure 7A), the docking score was found to be -7.378, indicating a moderate binding affinity of the ligand to the enzyme. The relatively low potential energy (–4.496 kJ/mol) suggests favorable thermodynamic stability of the complex. The RMS-derivative value of 0.114 Å shows a very low deviation, suggesting that the binding positions are reliable. The glide energy of -47.283 kcal/mol indicates good energy stabilization in the binding area. In contrast, the 2TBS/AHTPO interaction (Figure 7B) has a docking score of -7.953, indicating a stronger binding affinity with a more negative value. The glide energy is also lower at -49.782 kcal/mol, suggesting that the ligand is in a more favorable position during binding. However, this binding may be slightly less stable thermodynamically, as the potential energy is -1.107 kJ/mol, higher than the 1A0J/AHTPO system. Nevertheless, the RMS-derivative value of 0.119 Å shows a very low deviation, meaning both structures are stable in terms of binding positions.

As a result, the 2TBS/AHTPO interaction appears to be more advantageous in terms of binding affinity and energy stabilization. However, it has a slight disadvantage in terms of thermodynamic stability. Depending on the application context, 2TBS may be chosen if the strong binding affinity is a priority, while 1A0J may be preferred for a more stable system. The choice ultimately depends on the targeted biological activity and experimental conditions.

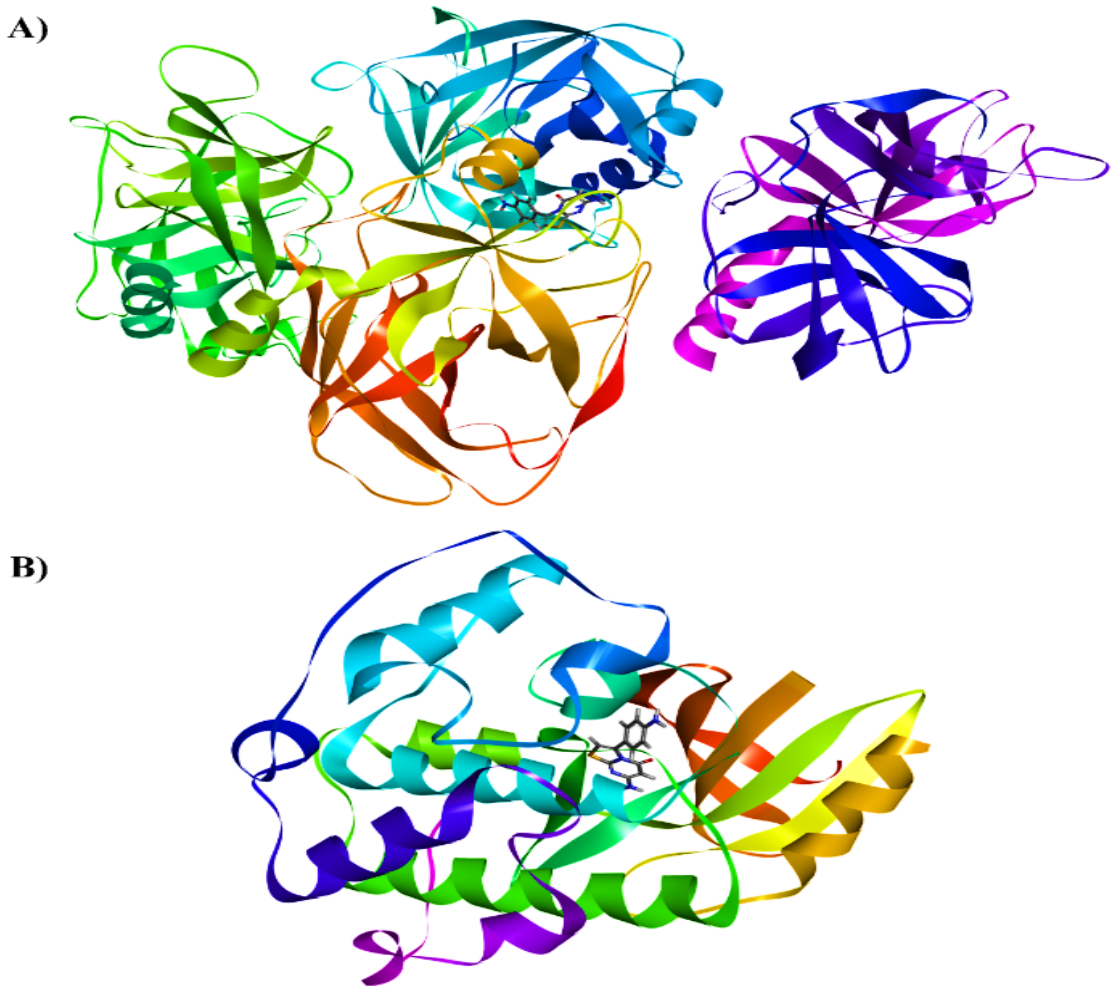


**Figure 7.** 3D schemes of the enzyme-ligand interaction of A) 1A0J/AHTPO and B) 2TBS/AHTPO (The three-dimensional interaction modes of AHTPO with 1A0J (A) and 2TBS (B). In the 2TBS complex, deeper burial of the ligand and stronger hydrogen bond networks correspond to the observed higher docking score and glide energy.)

When the 1A0J/AHTPO enzyme-ligand interaction (Figure 8) was examined in detail, Glutamine C:192 formed a short-range 2.87 Å conventional hydrogen bond with sulfur (S) in the ligand. This short-range hydrogen bonding indicates a strong interaction between the sulfur atom in the binding region of the ligand and Glutamine C:192, which contributes to the stability of the ligand and may play a critical role in the binding region. Tryptophan C:215 formed two distinct Pi-Pi T-shaped interactions with the Pyridazinone center at distances of 4.93 Å and 5.25 Å. Pi-Pi T-shaped interactions occur between aromatic rings, indicating a strong interaction between the ligand and the aromatic structures in the binding region.

The two separate distances suggest small variations in the strength of the interaction. Glutamine C:175 provided a short-range conventional hydrogen bond with the N-H group at a distance of 2.10 Å, indicating a very strong bond that plays a crucial role in stabilizing the binding site. Tyrosine C:217 formed a conventional hydrogen bond with the N-H group at 2.98 Å, as well as a Pi-Pi T-shaped interaction with the Pyridazinone center at 5.92 Å. The hydrogen bond with N-H emphasizes the importance of polar interactions in the binding site, while the Pi-Pi interaction at a larger distance suggests a weaker but still significant bonding between the ligand's aromatic ring and Tyrosine.

The two interactions at different distances may indicate the flexible role of Tyrosine in the binding site. Leucine C:99 formed a Pi-Alkyl interaction with the benzene center at 4.33 Å. This Pi-Alkyl interaction highlights the importance of hydrophobic interactions in the

binding site, which generally contribute to the stability of the binding complex. The ligand interacts with a variety of amino acids in the binding site through different bond types. Short-range hydrogen bonds (2.10 Å and 2.87 Å) and Pi-Pi T-shaped interactions indicate that the ligand is strongly localized within the binding site. Additionally, the presence of both polar and hydrophobic interactions further supports the ligand's conformation within the binding site.

When the 2TBS/AHTPO enzyme-ligand interaction (Figure 9) was examined, Aspartic Acid A:145 formed a short-range conventional hydrogen bond with the first N-H group at a distance of 2.11 Å. This short hydrogen bond indicates a strong interaction between the N-H group and Aspartic Acid, which plays a critical role in the binding region. Leucine A:83, on the other hand, bonded to the second N-H group with an even shorter distance of 1.82 Å, forming a conventional hydrogen bond. This exceptionally short bond is unique to this system and is thought to be an efficient binding at this region compared to the previous system.

Leucine A:134 was involved in two Pi-Alkyl interactions: one with the pyridazinone center at 4.47 Å and another with the S-C-N-C=C ring center at 4.64 Å. These two bonds are of similar strength, but the latter is slightly farther, indicating the ligand's diverse bonding patterns around the S-C-N-C=C ring. Valine A:18 formed Figure 10. Donor and acceptor regions are highlighted by standard color codes (purple for donors, green for acceptors. This color-coded surface allows for an easy distinction between the interaction types at the receptor's binding site. Regarding the aromatic surface, regions associated with sediment are displayed in orange, while areas bound to the stem are shown in blue. Aromatic moieties within the binding site significantly contribute to ligand stabilization through π–π interactions. The color distribution pattern on the H-bond surface is organized, indicating that the ligand is well-positioned within the receptor.

a long-range Pi-Alkyl interaction with the benzene center at 4.87 Å. While this bond might be weaker, it emphasizes the significance of aromatic interactions within the binding region. Isoleucine A:10 exhibited two Pi-Alkyl bonds: one with the pyridazinone center at 4.53 Å and another with the S-C-N-C=C ring center at 4.87

Å, similar to Leucine A:134. The fact that both Leucine A:134 and Isoleucine A:10 formed double bonds with similar rings suggests that this region of the ligand is an especially active binding site. This distinct double-bonding pattern was not observed in the previous system. Finally, Alanine A:31 formed a Pi-Alkyl bond with the pyridazinone center at the farthest distance of 5.01 Å. Although this bond is relatively weak, it underlines the importance of hydrophobic interactions on the aromatic structure of the ligand, contributing to the overall stability of the binding complex.

### 3.2.2. Interaction pattern surfaces on the receptor

Visual presentations showcasing the interactions and surface properties of the AHTPO/1A0J and AHTPO/2TBS enzyme-ligand systems are displayed. The 3D view highlights the interaction models involving AHTPO with the 1A0J and 2TBS enzymes. The hydrogen bonds (both acceptor and donor) and aromatic surface characteristics on the receptor are depicted in
This surface distribution indicates a dominantly polar character within the binding cavity [51]. Additionally, the analysis of the receptor molecules, scrutinized through molecular insertion techniques, highlights the specific interactions contributing to the overall stability of the ligand-receptor complex. The results show that the AHTPO/1A0J interaction exhibits a greater degree of efficacy in terms of surface interactions and color intensity, reflecting a stronger and more stable binding compared to the AHTPO/2TBS system.

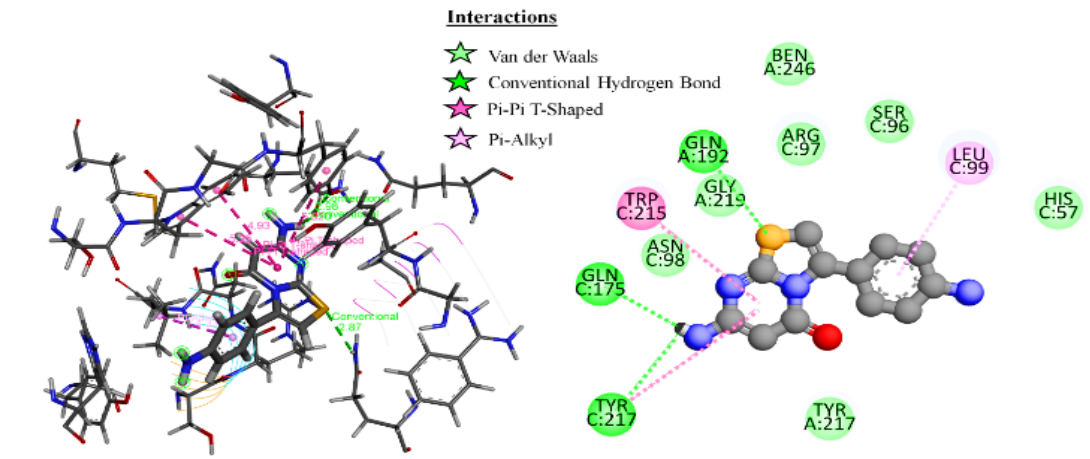


**Figure 8.** 2D scheme of the 1A0J/AHTPO enzyme-ligand interaction

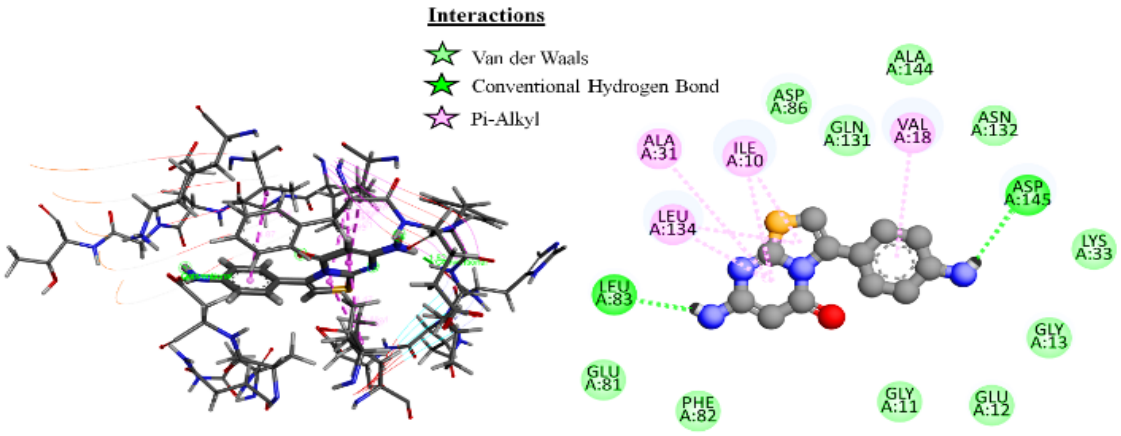


**Figure 9.** 2D scheme of 2TBS/AHTPO enzyme-ligand interaction

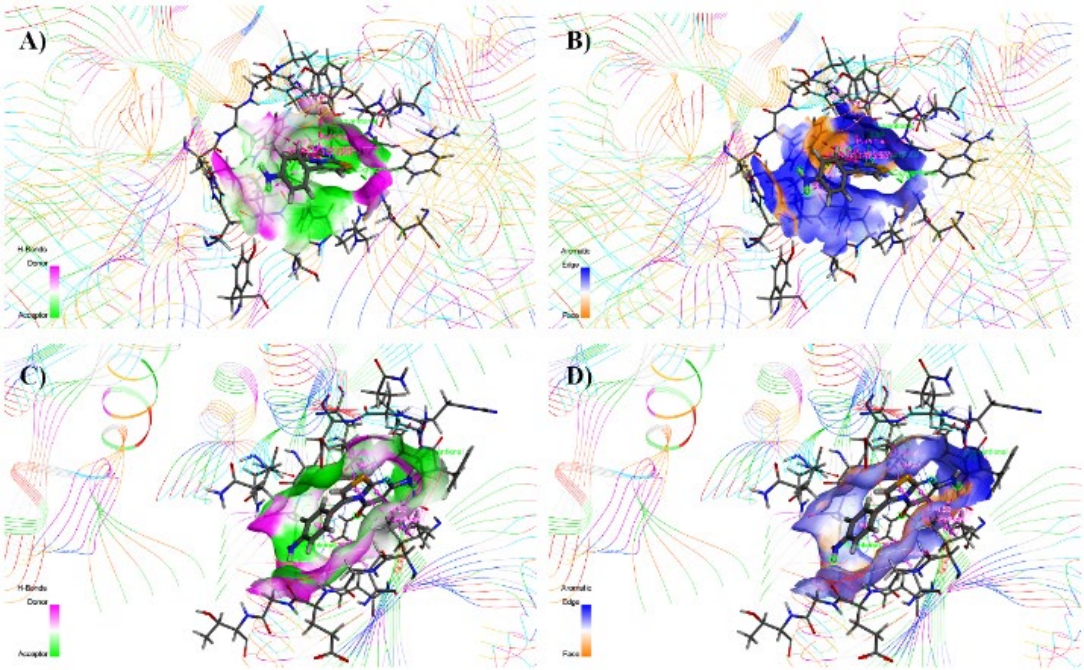


**Figure 10.** 3D view of the hydrogen bonds donor/acceptor surface (A, C) and the aromatic surface (B, D) model of interaction with 1A0J/AHTPO and 2TBS/AHTPO enzyme respectively (The hydrogen bond donor and acceptor surfaces (A, C) and aromatic surface distributions (B, D) emphasize the polar nature of the binding site. The more organized surface pattern in the 1A0J complex suggests improved enthalpic contributions to binding stability.)

### 3.3. Pharmacokinetic analysis

The structure of AHTPO was submitted to the SwissADME server to evaluate pharmacokinetic and physicochemical descriptors (in Table 3). According to Lipinski's "rule of five," compounds should not exceed 10 hydrogen bond acceptors (HBAs) or 5 hydrogen bond donors (HBDs) [52]. The compound in question adheres to these criteria, as evidenced by the calculated data for HBAs and HBDs.

The topological polar surface area (tPSA) is a critical parameter for assessing the impact of polar groups on membrane permeability, and it should not exceed 140 Å² to facilitate blood-brain barrier (BBB) penetration. The tPSA for this compound was found to be within the acceptable range. However, the gastrointestinal (GI) absorption rate was identified as poor, and the compound is not expected to penetrate the BBB. Furthermore, the AHTPO meets the criteria set by Lipinski, Veber, and Egan [53]. That is, the potential of AHTPO as an effective treatment option for targeted diseases has been expressed. The bioavailability radar plot (Figure 11) indicates that the compound resides within the optimal physicochemical space for oral drug candidates.

**Table 3.** Physicochemical and lipophilicity of the most active AHTPO using SwissADME software

| | | | |
|---|---|---|---|
| **Molecular Weight** | 258.06 | **f-Char** | 0 |
| **Density** | 1.061 | **n-Rig** | 17 |
| **n-HA** | 5 | **Flexibility** | 0.059 |
| **n-HD** | 4 | **Stereo-Centers** | 0 |
| **n-Rot** | 1 | **TPSA** | 86.41 |
| **nRing** | 3 | **Log-S** | -2.857 |
| **Max-Ring** | 9 | **Log-P** | 1.160 |
| **n-Het** | 6 | **Log-D** | 1.451 |

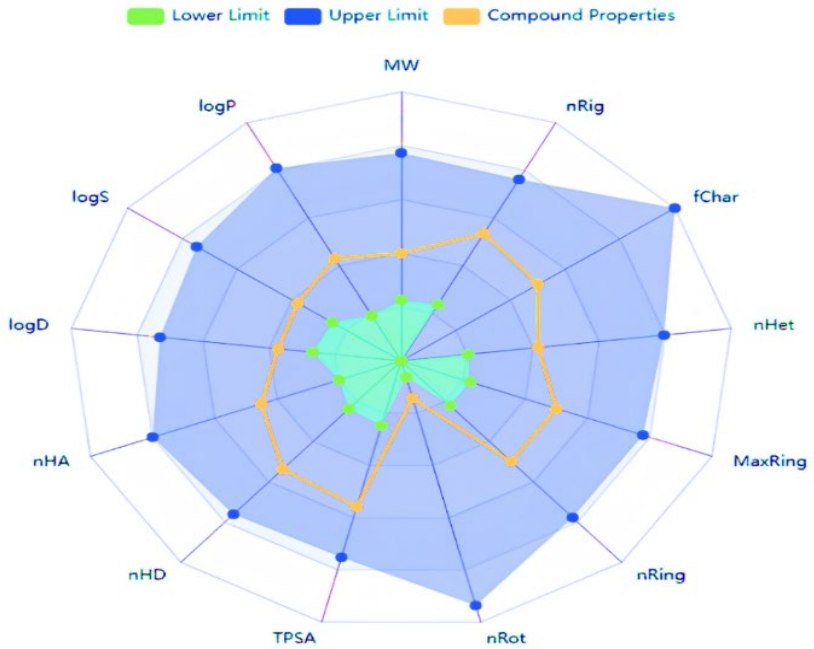


**Figure 11.** Color regions and pharmacological parameters of the compound AHTPO (Depicts the bioavailability radar plot for AHTPO. The compound lies within the optimal zone for lipophilicity and molecular size, although minor deviation in polarity may limit gastrointestinal absorption.)

This zone highlights the specific ranges of parameters such as size, lipophilicity, polarity, and solubility, which are essential for the efficient absorption and bioavailability of compounds when administered orally. By identifying these ideal characteristics, researchers can more effectively assess the potential of new compounds for therapeutic

applications, ensuring they possess the necessary properties for effective absorption and distribution within the body.

Revealed that AHTPO meets major pharmacokinetic criteria, including Lipinski's rule of five. However, it may exhibit limitations in gastrointestinal absorption and blood-brain barrier permeability. Despite these challenges, its topological polar surface area (tPSA = 86.41 Å$^2$) and favorable physicochemical properties indicate potential for further optimization as a drug candidate.

## 4.Conclusion

Molecular docking results demonstrated that AHTPO exhibited strong binding affinity with the 2TBS enzyme (docking score: -7.953; glide energy: -49.782 kcal/mol), while the 1A0J complex showed greater thermodynamic stability (-4.496 kJ/mol). Low RMS-derivative values in both systems confirmed the reliability of the binding poses. DFT calculations revealed that AHTPO possesses favorable electronic characteristics, including high dipole moment, polarizability, and a shown HOMO–LUMO gap (3.5640-4.4652 eV), indicating balanced reactivity in biological contexts.

ADME analysis suggested pharmacological applicability, although limited gastrointestinal absorption and blood–brain barrier permeability were observed. Collectively, these findings support AHTPO's potential as a bioactive compound with relevance to drug discovery and enzyme-targeted applications.

## Article Information Form

### *Authors' Contribution*

EAT: Data Collection, Writing, Literature Review; AAT: Concept/Design, Data Analysis, Writing, Critical Review of Content, Literature Review; ÜY: Technical Support; Critical Review of Content, Literature Review.

### *The Declaration of Conflict of Interest/ Common Interest*

No conflict of interest or common interest has been declared by authors.

### *Artificial Intelligence Statement*

No artificial intelligence tools were used while writing this article.

### *Copyright Statement*



## References

[1] D. Cai, Z. H. Zhang, Y. Chen, X. J. Yan, S. T. Zhang, L. J. Zou, L. H. Meng, F. Li, B. J. Fu, "Synthesis of some new thiazolo[3,2a]pyrimidine derivatives and screening of their in vitro antibacterial and antitubercular activities," Medicinal Chemistry Research, vol. 25, pp. 292-302, 2016.

[2] J. C. Roach, "A clade of trypsins found in cold-adapted fish," Proteins: Structure, Function, and Bioinformatics, vol. 47, pp. 31-44, 2002.

[3] A. Muhlia-Almazán, A. Sánchez-Paz, F. L. García-Carreño, "Invertebrate trypsins: A review," J Comp Physiol B, vol. 178, pp. 655-72, 2008.

[4] R. T. Azuma, "Survey of augmented reality," Presence: Teleoperators and Virtual Environments, vol. 6, no. 4, pp. 355-385, 1997.

[5] O. Gon, P. C. Heemstra, "Fishes of the southern ocean," Reviews in Fish Biology and Fisheries, vol. 2, pp. 344-345, 1990.

[6] G. Bianchi, "Sustainable fisheries within an LME context," Environmental Development, vol. 17, no. 1, pp. 182-192, 2016.

[7] P. C. Agu, C. A. Afiukwa, O. U. Orji, E. M. Ezeh, I. H. Ofoke, C. O. Ogbu, E. I. Ugwuja, P. M. Aja, "Molecular docking as a tool for the discovery of molecular targets of nutraceuticals in diseases management," Scientific Reports, vol. 13, p. 13398, 2023.

[8] S. Demirel, A. Güller, M. Usta, Z. Kurt, G. Korkmaz, “Coat protein of alfalfa mosaic alfamovirus (AMV) from Türkiye: Genetic inference and in silico docking analysis for potential antiphytoviral purposes. Notulae Botanicae Horti Agrobotanici Cluj-Napoca,” vol. 52, no. 1, 2024.

[9] U. S. T. A. Mustafa, A. Güller, S. Demirel, G. Korkmaz, K. U. R. T. Zeynelabidin, “New insights into tomato spotted wilt orthotospovirus (TSWV) infections in Türkiye: Molecular detection, phylogenetic analysis, and in silico docking study,” Notulae Botanicae Horti Agrobotanici Cluj-Napoca, vol. 51, no. 3, pp. 13245-13245, 2023.

[10] S. Choudhuri, M. Yendluri, S. Poddar, A. Li, K. Mallick, S. Mallik, B. Ghosh, “Recent advancements in computational drug design algorithms through machine learning and optimization,” Kinases and Phosphatases [Online], pp. 117-140, 2023.

[11] C. Yang, E. A. Chen, Y. Zhang, “Protein-Ligand Docking in the Machine-Learning Era,” Molecules, vol. 27, 2022.J.

[12] Abdullah, A. A. Tanriverdi, A. A. Khan, S. J. Lee, J. B. Park, Y. S. Kim, U. Yildiko, K. Min, M. Alam, “Selenium-substituted conjugated small molecule: Synthesis, spectroscopic, computational studies, antioxidant activity, and molecular docking,” Journal of Molecular Structure, vol. 1304, p.137694, 2024.

[13] R. Tiwari, K. Mahasenan, R. Pavlovicz, C. Li, W. Tjarks, “Carborane clusters in computational drug design: A Comparative docking evaluation using AutoDock, FlexX, Glide, and Surflex," Journal of chemical information and modeling, vol. 49, pp. 1581-9, 2009.

[14] C. George Priya Doss, C. Chakraborty, V. Narayan, D. Thirumal Kumar, “Computational Approaches and Resources in Single Amino Acid Substitutions Analysis Toward Clinical Research,” In Advances in Protein Chemistry and Structural Biology, Donev, R., Ed. Chapter Ten -vol. 94, pp. 365-423, Academic Press: 2014.

[15] K. W. Lexa, H. A. Carlson, “Protein flexibility in docking and surface mapping,” Q Rev Biophys, vol. 45, pp. 301-43, 2012.

[16] N. K. Borah, Y. Tripathi, A. Tanwar, D. Tiwari, A. Sinha, S. Sharma, N. Jabalia, R. J. Mani, S. Santoshi, H. Bansal, “Artificial intelligence-powered molecular docking,” In Artificial Intelligence and Machine Learning in Drug Design and Development, pp. 157-188, 2024.

[17] H. K. Schrøder, N. P. Willassen, A. O. Smalås, “Structure of a Non-psychrophilic trypsin from a cold-adapted fish species,” Acta Crystallographica Section D, vol. 54, pp. 780-798, 1998.

[18] A. O. Smalås, E. S. Heimstad, A. Hordvik, N. P. Willassen, R. Male, “Cold adaption of enzymes: Structural comparison between salmon and bovine trypsins,” Proteins: Structure, Function, and Bioinformatics, vol. 20, pp. 149-166, 1994.

[19] S. O. Oselusi, P. Dube, A. I. Odugbemi, K. A. Akinyede, T. L. Ilori, E. Egieyeh, N. R. S. Sibuyi, M. Meyer, A. M. Madiehe, G. J. Wyckoff, S. A. Egieyeh, “The role and potential of computer-aided drug discovery strategies in the discovery of novel antimicrobials,” Computers in Biology and Medicine, vol. 169, p. 107927, 2024.

[20] S. Racioppi, P. Lolur, P. Hyldgaard, M. Rahm, “A density functional theory for the average electron energy,” Journal of Chemical Theory and Computation, vol. 19, pp. 799-807, 2023.

[21] K. Gören, M. Bağlan, Ü. Yıldıko, “Analysis by DFT, adme and docking studies of N'-(4-Hydroxy-3-Methoxybenzylidene) Naphtho [2, 3-B] Furan-2-Carbohydrazide,” ESTU Science, vol. 13, no. 1, pp. 7-23, 2025.

[22] A. J. Cohen, P. Mori-Sánchez, W. Yang, "Challenges for Density Functional Theory," Chemical Reviews, vol. 112, pp. 289-320, 2012.

[23] U. Yildiko, A. A. Tanriverdi, "A novel sulfonated aromatic polyimide synthesis and characterization: Energy calculations, QTAIM simulation study of the hydrated structure of one unit," Bulletin of the Korean Chemical Society, vol. 43, pp. 822-835, 2022.

[24] M. Bursch, J. M. Mewes, A. Hansen, S. Grimme, "Best-Practice DFT Protocols for Basic Molecular Computational Chemistry," Angewandte Chemie International Edition, vol. 61, p. e202205735, 2022.

[25] K. Gören, Ü. Yıldıko, "Aldose reductase evaluation against diabetic complications using ADME and molecular docking studies and DFT calculations of spiroindoline derivative molecule," Süleyman Demirel University Journal of Natural and Applied Sciences, vol. 28, pp. 281-292, 2024.

[26] C. D. Gandhi, P. Sappidi, "Molecular Dynamics Simulation Study on the Structural and Thermodynamic Analysis of Oxidized and Unoxidized Forms of Polyaniline," The Journal of Physical Chemistry B, vol. 128, pp. 10735-10748, 2024.

[27] Ü. Yildiko, A. Ç. Ata, A. A. Tanriverdi, İ. Çakmak, "Investigation of novel diethanolamine dithiocarbamate agent for RAFT polymerization: DFT computational study of the oligomer molecules," Bulletin of Materials Science, vol. 44, p. 186, 2021.

[28] A. I. Osman, A. Ayati, P. Krivoshapkin, B. Tanhaei, M. Farghali, P. S. Yap, A. Abdelhaleem, "Coordination-driven innovations in low-energy catalytic processes: Advancing sustainability in chemical production," Coordination Chemistry Reviews, vol. 514, p. 215900, 2024.

[29] K. Gören, M. Bağlan, Ü. Yıldıko, "Antimicrobial, and Antitubercular Evaluation with ADME and Molecular Docking Studies and DFT Calculatıons of (Z)-3-((1-(5-amino-1, 3, 4-thiadiazol-2-yl)-2-Phenylethyl) imino)-5-nitroindolin-2-one Schiff Base," The Black Sea Journal of Sciences, vol. 14, pp. 1694-1708, 2024.

[30] M. Frisch, F. Clemente, M. J. Frisch, G. W. Trucks, H. B. Schlegel, G. E. Scuseria, M. A. Robb, J. R. Cheeseman, G. Scalmani, V. Barone, B. Mennucci, G. A. Petersson, H. Nakatsuji, M. Caricato, X. Li, H. P. Hratchian, A. F. Izmaylov, J. Bloino and G. Zhe, Gaussian 9.

[31] Schrödinger Release 2017-3: Schrödinger Suite 2017-3 Protein Preparation Wizard, Epik, Schrödinger, LLC, New York, NY, Impact, Schrödinger, LLC, New York, NY, 2017; LigPrep, Schrödinger, LLC, New York, NY, 2017; Prime, Schrödinger, LLC, New York, NY, 2017; QikProp, Schrödinger, LLC, New York, NY, 2017.

[32] Ü. Yildiko, F. Türkan, A. A. Tanriverdi, A. C. Ata, M. N. Atalar, İ. Cakmak, "Synthesis, enzymes inhibitory properties and characterization of 2- (bis (4-aminophenyl) methyl) butan-1-ol compound: Quantum simulations, and in-silico molecular docking studies," Journal of the Indian Chemical Society, vol. 98, p.100206, 2021.

[33] SYSTÈMES BDSD, BIOVIA Corporate Europe, BIOVIA 334 Cambridge Science Park, Cambridge CB4 0WN, England, 2016.

[34] L. Fu, S. Shi, J. Yi, N. Wang, Y. He, Z. Wu, J. Peng, Y. Deng, W. Wang, C. Wu, A. Lyu, X. Zeng, W. Zhao, T. Hou, D. Cao, "ADMETlab 3.0: An updated comprehensive online ADMET prediction platform enhanced with broader coverage, improved performance, API functionality and decision support," Nucleic Acids Research, vol. 52, pp. W422-W431, 2024.

[35] M. Quirós, S. Gražulis, S. Girdzijauskaitė, A. Merkys, A. Vaitkus, "Using SMILES strings for the description of chemical connectivity in the Crystallography Open Database," Journal of Cheminformatics, vol. 10, p. 23, 2018.

[36] E. Akbas, E. Ergan, E. Sahin, S. Ekin, M. Cakir, Y. Karakus, "Synthesis, characterization, antioxidant properties and DFT calculation of some new pyrimidine derivatives," Phosphorus, Sulfur, and Silicon and the Related Elements vol. 194, pp. 796-802, 2019.

[37] B. Kartal, A. A. Tanriverdi, U. Yildiko, A. T. Tekes, I. Çakmak, "Polyimide synthesis and characterizations: DFT-assisted computational studies on structural units," Iranian Polymer Journal, 2024.

[38] A. Ç. Ata, Ü. Yildiko, A. A. Tanriverdi, R. Ebiri, E. Yiğit, İ. Orak, İ. Cakmak, "Two-step novel aromatic polyimide synthesis and characterization: Survey of energy calculations and diode applications," Journal of Applied Polymer Science, vol. 140, p. e53689, 2023.

[39] U. Yildiko, A. A. Tanriverdi, "Synthesis and characterization of pyromellitic dianhydride based sulfonated polyimide: Survey of structure properties with DFT and QTAIM," Journal of Polymer Research, vol. 29, p. 19, 2021.

[40] K. Gören, E. Çimen, V. Tahiroğlu, Ü. Yıldıko, "Moleculer docking and theoretical analysis of the (E)-5-((Z)-4-methylbenzylidene)-2-(((E)-4-methylbenzylidene) hydrazineylidene)-3-phenylthiazolidin-4-one Molecule," Bitlis Eren Üniversitesi Fen Bilimleri Dergisi, vol. 13, pp. 659-672, 2024.

[41] S.R. Mannopantar, B. Maheshkumar, D. Ramesh, A. S. Lalasangi, H. H. Bendigeri, M. N. Kalasad, V. K. Kulkarni, "Effect of Ag2O nanoparticles on the excited state dipole moment of a novel BMNFC molecules through solvatochromic shift method," Spectrochimica Acta Part A: Molecular and Biomolecular Spectroscopy, vol. 326, p. 125190, 2025.

[42] M. Włodarska, B. Mossety-Leszczak, "DFT studies of selected epoxies with mesogenic units–impact of molecular structure on electro-optical response," International Journal of Molecular Sciences, vol. 22, p. 3424, 2021.

[43] N. Serin, T. Serin, B. Ünal, "The interaction of the dipole moment of the water molecule with the interface states of the cuprous oxide/cupric oxide junction," Turkish Journal of Physics, vol. 24, no. 2, pp. 137-142, 2000.

[44] J. R. P. S. Souza, G. V. S. Mota, H. R. Bitencourt, S. G. Moreira, C. M. R. Remédios, "Spectroscopic characterization (FT-IR, RAMAN and UV–VIS), thermogravimetric analysis, XPD and DFT calculations of highly stable hydroxy-functionalized chalcone: (2E)-1-(4-hidroxyphenyl)-3-(4-methoxyphenil)-prop-2-en-1-one," Journal of Molecular Structure, vol. 1295, p. 136702, 2024.

[45] N. Akter, S. Saha, M. A. Hossain, K. M. Uddin, A. R. Bhat, S. Ahmed, S. M. A. Kawsar, "Acylated glucopyranosides: FTIR, NMR, FMO, MEP, molecular docking, dynamics simulation, ADMET and antimicrobial activity against bacterial and fungal pathogens," Chemical Physics Impact, vol. 9, p. 100700, 2024.

[46] K. Gören, M. Bağlan, Ü Yıldıko, "Melanoma cancer evaluation with ADME and molecular docking analysis, DFT calculations of (E)-methyl 3-(1-(4-methoxybenzyl)-2, 3-dioxoindolin-5-yl)-acrylate molecule," Journal of the Institute of Science and Technology, vol. 14, pp. 1186-1199, 2024.

[47] M. Guo, M. Ji, W. Cui, "Theoretical investigation of HER/OER/ORR catalytic activity of single atom-decorated graphyne by DFT and comparative DOS analyses," Applied Surface Science, vol. 592, p. 153237, 2022.

[48] Z. A. Abdallah, A. M. Abdelfattah, A. A. M. Ahmed, "Benzo[6,7]cyclohepta[1,2-d]pyrazolo[1,5-a]pyrimidines: Regioselective synthesis of a novel ring system, DFT-based NMR prediction, local reactivity indexes, and MEP analysis," Journal of Molecular Structure, vol. 1321, p. 140030, 2025.

[49] T. Pantsar, A. Poso, "Binding Affinity via Docking: Fact and Fiction," Molecules [Online], vol. 23, p. 1899, 2018.

[50] D. G. Solgun, A. A. Tanriverdi, U. Yildiko, M. S. Ağirtaş, "Synthesis of axially silicon phthalocyanine substituted with bis- (3,4-dimethoxyphenethoxy) groups, DFT and molecular docking studies," Journal of Inclusion Phenomena and Macrocyclic Chemistry, vol. 102, pp. 851-860, 2022.

[51] K. Basu, E. S. Brielle, I. T Arkin, "Hydrogen bond strengthens acceptor group: The curious case of the C–H···O=C Bond," International Journal of Molecular Sciences [Online], vol. 25, p. 8606, 2024.

[52] C. A. Lipinski, "Lead- and drug-like compounds: The rule-of-five revolution," Drug Discovery Today: Technologies, vol. 1, pp. 337-341, 2004.

[53] C. Doak Bradley, B. Over, F. Giordanetto, J Kihlberg, "Oral Druggable Space beyond the Rule of 5: Insights from drugs and clinical candidates," Chemistry & Biology, vol. 21, pp. 1115-1142, 2014.